Finite Element Analysis of Three Dimensional Complex Scatterers in Layered Media

Xuewei Ping [1], Xinghui Yin [1], Li Li [1], Changli Li [1], and Qingbo Li [2]

[1] College of Computer and Information Engineering
HoHai University, Nanjing, 211100, Jiangsu, China
xwping@hhu.edu.cn, xhyin@hhu.edu.cn, lili_lee@hhu.edu.cn, charlee@hhu.edu.cn

[2] Jiangsu Key Construction Laboratory of Modern Measurement Technology and Intelligent System
Huaiyin Normal University, Huai'an, 223300, China
qingboli12@126.com

Abstract **─** In this paper, an efficient three-dimensional finite-element method (FEM) is introduced to study the scattering from complex three-dimensional objects in the layered media. The proposed method is valid to targets which are located either close to or far away from the media interface. Furthermore, the interface can be either a planar or rough surface in the computational domain. To improve efficiency, the preconditioned conjugate gradient method for normal equations (CGN) are proposed to solve the FEM linear system. Numerical examples are presented to demonstrate the accuracy and efficiency of the presented method.

Index Terms **─** Complex objects, electromagnetic scattering, finite element method, layered media.

I. INTRODUCTION

The investigation of complex electromagnetic (EM) scattering characteristic of targets in the layered media has been of interest due to extensive applications, such as near-surface geophysical exploration, investigation of automobiles and other vehicles over road or terrain surfaces and landmine detection, etc. A viable and efficient way to deal with this kind of problem is to use analytical or numerical simulation methods. Ref. [1] developed the analytical expressions for calculating scattering from buried homogeneous objects in a low-contrast situation for several geometries. For complex media or complex structures, numerical methods have to be used. The method of moment (MOM)-based techniques [2-5], such as the multilevel fast multipole algorithm (MLFMA) [2-3], the conjugate gradient method and fast Fourier transform (CG-FFT) [4], are efficient ways for the numerical simulations of the perfectly electrical conducting (PEC) objects or homogeneous dielectric objects. The principle challenge of MOM to solve the scattering problems in half space or layered media is the evaluation of the spatial dyadic Green's function (SDGF), each component of which is expressed in an oscillatory Sommerfeld integration. Furthermore, these methods is most suitable for structures only contain perfectly conductors, and are less efficient in solving complex media.

Another efficient method to deal with scattering problems in layered media is the finite-difference time-domain (FDTD) method [6-8]. The deficiency of FDTD is that the stair-cased meshing can lead to inaccuracy in modeling complex geometries, though the application of conformal meshes can alleviate this deficiency for some extent. For problems containing complex structures or dispersion medium, the finite element method is the most suitable method. In this paper, a three-dimensional (3D) tangential vector finite element method (TVFEM) is introduced to simulate the scattering characteristics of targets in the presence of air-earth interface.

The advantage of TVFEM is that it can cope with material discontinuities as well as complex structures in a natural way. In the past a few decades, TVFEM has been paid much attention and have developed rapidly in theory and practical applications [9-12]. However, in most of the published FEM research contributions, the influence of the background medium is rarely considered. Some investigations on FEM simulation of buried scatterers are as follows. In [13], a 2D planar anisotropic perfectly matched layer for the FEM mesh truncation tool was investigated for electromagnetic scattering by buried objects. However, the detailed FEM process to simulate buried objects was not given. In [14], a 2-D FEM model is set up based on the Monte Carlo method for predicting the statistical properties of the electromagnetic scattering from objects on or above random rough sea surfaces. In [15-19], the combination of finite-element and the boundary-integral (FEBI) method are proposed. This kind of methods can solve complex structures. However, the sparsity of the FEM matrix will be destroyed, which will make the solution

Submitted On: April 18, 2016
Accepted On: October 25, 2016

of the FEM linear system difficult.

In this paper, we propose an efficient 3D FEM based on scattered electric field to solve the scattering problems in multi-layered media. From the FEM process given below, it can be seen that the computational efficiency of this method for targets in multi-layered media is comparable with that for targets in free space.

II. FORMULATION

The FEM computational domain for a typical scattering problem in layered media is shown in Fig. 1. The scattering target is formed with arbitrary media, such as inhomogeneous dielectrics, metals, etc. The permittivity and permeability of the media within any point of the computational domain are denoted as ε_r and μ_r respectively. In order to truncate the FEM computational domain, the outer boundary of the scattering target is lined with absorbing perfectly matched layers (PMLs). In order to consider the affection of the air-earth interface to the scattered field, the interface has to be included in the computational domain. For simplicity, the computational domain is denoted as Ω, the region occupied by the scatterer is denoted as Ω_{sc}, the bounding surface of the scatterer is denoted as S, the normal vector of the bounding surface is *n*. For simplicity, only plane wave is discussed in this paper. The incident wave is denoted as E_i, the reflected and transmitted fields due to E_i is denoted as E_r and E_t. For simplicity, the propagation direction of incident wave is supposed to be in the xz plane, and the incident angle is θ_i.

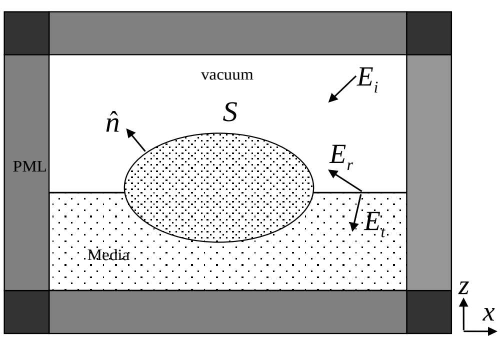

Fig. 1. Illustration of the FEM computational domain of scattering targets in layered media.

For TE modes, the incident, reflected and transmitted fields can be expressed as follows:

$$\begin{aligned} E_i &= E_0 \bar{y}\, e^{-jk_0(x\cdot\sin\theta_i + z\cdot\cos\theta_i)} \\ E_r &= R^{TE} E_0 \bar{y}\, e^{-jk_0(x\cdot\sin\theta_i - z\cdot\cos\theta_i)} \\ E_t &= T^{TE} E_0 \bar{y}\, e^{-jk_0\sqrt{\varepsilon_r\mu_r}(x\cdot\sin\theta_t + z\cdot\cos\theta_t)} \end{aligned} \quad . \tag{1}$$

For TM modes:

$$\begin{aligned} E_i &= E_0\, e^{jk_0(x\cdot\sin\theta_i + z\cdot\cos\theta_i)} \left(\cos\theta_i \bar{x} - \sin\theta_i \bar{z}\right) \\ E_r &= -R^{TM} E_0\, e^{jk_0(x\sin\theta_i - z\cos\theta_i)} \left(\cos\theta_i \bar{x} + \sin\theta_i \bar{z}\right) \\ E_t &= T^{TM} E_0\, e^{jk_0\sqrt{\varepsilon_r\mu_r}(x\cdot\sin\theta_t + z\cdot\cos\theta_t)} \left(\cos\theta_t \bar{x} - \sin\theta_t \bar{z}\right) \end{aligned} \quad . \tag{2}$$

If the propagation direction of incident wave is not in the xz plane, the expression of E_i, E_r and E_t can be obtained by Equation (1) and Equation (2) through coordinate rotation. The equivalent incident electric field on the surface of the targets above the air-earth interface can be obtained with the reflection coefficient approximation formulation:

$$E^{inc} = E_i + E_r \, . \tag{3}$$

And the equivalent incident electric field obtained with the reflection coefficient approximation below the air-earth interface is:

$$E^{inc} = E_t \, . \tag{4}$$

To derive the FEM formulation, the vector wave equation based on electric field is written:

$$\nabla \times \left(\mu_r^{-1} \cdot \nabla \times E\right) - k_0^2 \varepsilon_r \cdot E = 0 \, , \tag{5}$$

where $k_0 = \omega\sqrt{\mu_0\varepsilon_0}$, E is the total electric field, which can be decomposed into two parts:

$$E = E^{sc} + E^{inc} \, , \tag{6}$$

where E^{sc} is the scattered field of the targets, E^{inc} is the equivalent incident field given by Equation (3) and Equation (4).

In FEM simulation, it is more efficient to work with the scattered electric field than the total electric field E. By substituting (6) into Equation (5), one obtains:

$$\begin{aligned} &\nabla \times \left(\mu_r^{-1} \cdot \nabla \times E^{sc}\right) - k_0^2 \varepsilon_r \cdot E^{sc} \\ &= -\nabla \times \left(\mu_r^{-1} \cdot \nabla \times E^{inc}\right) + k_0^2 \varepsilon_r \cdot E^{inc} \end{aligned} \, . \tag{7}$$

According to the generalized variational principle, the functional pertinent to the scattering field is written [9]:

$$\begin{aligned} F(E^{sc}) = \frac{1}{2}\int_{\Omega} & [(\nabla \times E^{sc}) \cdot \mu_r^{-1} \cdot (\nabla \times E^{sc}) \\ & - k_0^2 E^{sc} \cdot \varepsilon_r \cdot E^{sc}] dV \\ & + \int_{\Omega_{sc}} [(\nabla \times E^{sc}) \cdot \mu_r^{-1} \cdot (\nabla \times E^{inc}) \\ & - k_0^2 E^{sc} \cdot \varepsilon_r \cdot E^{inc}] dV \\ & + \int_{\Gamma_{sc}} \left[E^{sc} \cdot \hat{n} \times \nabla \times E^{inc}\right] dS \end{aligned} \, . \tag{8}$$

Note that in the derivation of Equation (8), the following formulation is used:

$$\nabla \times \nabla \times E^{inc} - k_0^2 E^{inc} = 0 \, . \tag{9}$$

In this paper, tetrahedron elements are used for mesh discretization, the scattered field within each element is expanded with H_0(curl) basis.

III. THE PRECONDITIONED CGN SOLVER

Using the Ritz variational or Galerkin method [9], a large sparse algebraic linear system is obtained, which can be written into the following form:

$$\mathbf{A}x = b, \tag{10}$$

with $\boldsymbol{A} \in \boldsymbol{C}^{n\times n}$, $b,\ x \in \boldsymbol{C}^{n}$.

As is well known, the efficiency of FEM is mainly determined by the efficiency of solving Equation (10). There are many different methods to solve Equation (10) [20-24]. For small problems, the multifrontal method always has satisfactory behavior. However, iterative methods are better choice, as which can save a great deal of memory compared with direct methods. In this paper, the preconditioned conjugate gradient for normal equations (PCGN) method [9] are proposed for the finite element solution of scattering problems. The FSAI-CGN solver proposed in [24] is especially investigated to solve the FEM linear systems generated from targets in the presence of air-earth interface. Though this method is less efficient than ICCG [23], however, it is very stable. What's more, it is very suitable for parallel, which is an important property as the ability to solve large 3D FEM linear systems is most meaningful.

IV. FURTHER DISCUSSIONS

In theory, the above process for the formation of the FEM linear system is applicable for any scatterers in the presence of air-earth interface. However, when the targets are placed far away from the interface, the whole computational domain will be very large and make the method very inefficient or even infeasible because both the targets and the region near the interface have to be included in the FEM computational domain. To overcome this difficulty, the simplified FEM model in Fig. 2 is recommended.

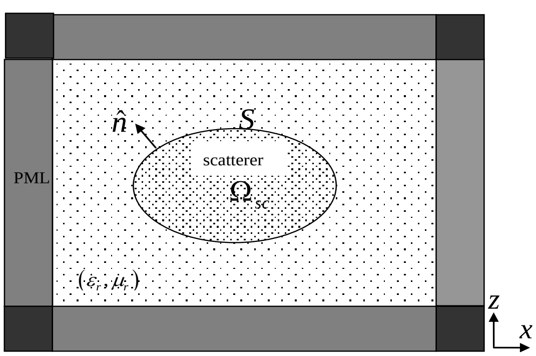

Fig. 2. Illustration of the FEM computational domain when scattering targets is far away from the interface.

In this model, only the region near the targets is included in the computational domain, the air-earth interface is not necessarily included. However, the total incident wave is still computed with Equations (3) and (4). In this model, the contribution of the interface to the scattered field is omitted. When the targets are placed far away from the interface, this simplification won't influence the accuracy of FEM. However, the efficiency is greatly enhanced.

In the deduction of the FEM formulations, the air-earth interface is assumed to be infinitely large and planar. However, this is not always the case in practical applications. In fact, the air-earth interface is not necessarily planar in the proposed algorithm. Let's see the problem shown in Fig. 3. In this problem, the interface above the scattering target is full of bumps and hollows; in other places, the interface is planar.

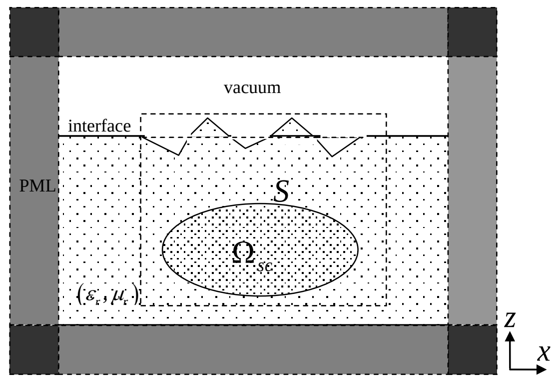

Fig. 3. Illustration of the FEM model when the air-earth interface is not planar in the computational domain.

This kind of problem can also be dealt with using the proposed method by treating the earth above the interface and the air below the interface as scatterers. If the far field and RCS are computed, the integration will be done on the surface expressed with the dashed line. If the air-earth interfaces are all rough in any places, the proposed method is no longer applicable because the excitation wave on the scatterers can no longer be expressed by Equation (3) and Equation (4).

In the next section, the proposed method is applied to analyze the scattering characteristics of some targets in the existence of layered media to validate the accuracy of the proposed method.

V. NUMERICAL RESULTS

The first example is the scattering characteristics of a perfectly conducting (PEC) sphere with radius 1.0λ half buried in the earth. The electric constant of the earth is $\varepsilon_r = 2.0 - 0.1j$, $\mu_r = 1.0$. The illustrated wireframe of the FEM model for this problem in the xz plane is shown in Fig. 4. In order to apply FEM simulation, the problem is divided into 550008 tetrahedrons, with the average mesh size 0.05λ. The number of FEM unknown edges generated is 676788. To validate the accuracy of 3D FEM, this problem is simulated with the software FEKO, in which MOM combined with exact Sommerfeld integration is selected. The mesh in FEKO are also chosen to be 0.05λ, and the number of triangle meshes is 13868. In Fig. 5, the VV polarized bi-static radar cross sections of the PEC sphere is computed, the incident angle is $\theta=0^o, \varphi=0^o$. The comparison of FEM results with the simulated results by FEKO is depicted in the figure. Good agreements are found in both figures.

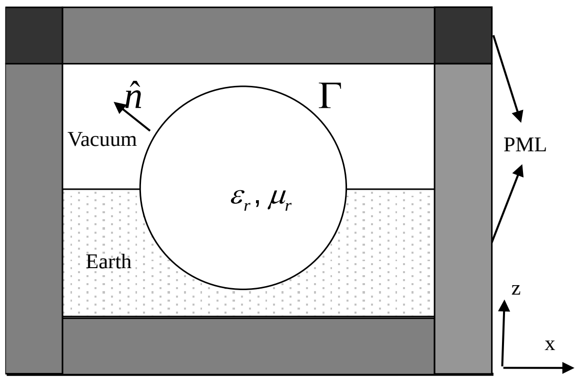

Fig. 4. Illustration of the FEM computational domain of a PEC sphere half buried in the earth.

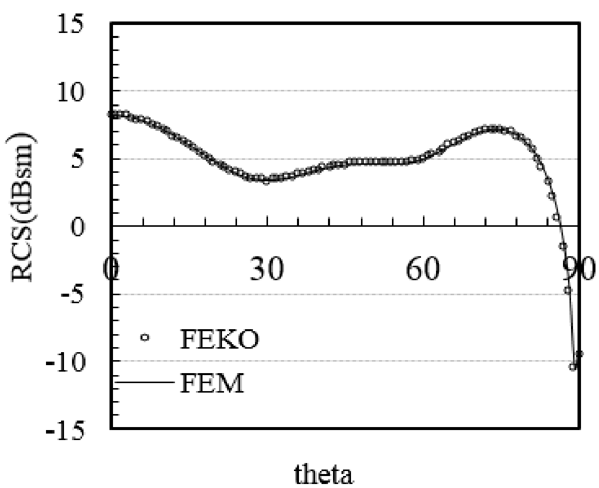

Fig. 5. Bi-static radar cross sections of the PEC sphere half buried in the earth.

In solving the finite element system, the comparison of different preconditioned CGN solvers are made. The convergence curves of D-CGN, SSOR-CGN and FSAI-CGN are shown in Fig. 6. In Table 1, the CPU time and memory are listed. From the table, it can be seen that the finite element method is more efficient than FEKO in solving this problem. It should be noted that, as the FEM matrix is symmetric, only half should be stored. The SSOR preconditioner is not necessary to be stored as it is the same as half of the matrix.

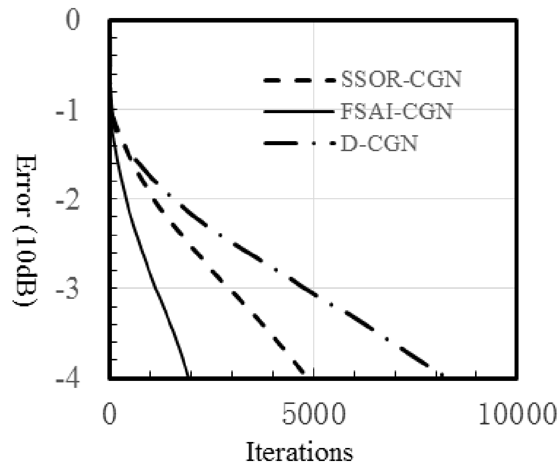

Fig. 6. Iterative behaviors of different solvers for finite element simulation of the PEC sphere half buried in the earth.

Table 1: CPU time and memory comparison of different methods

Solver		CPU Time (sec)	Memory (MB)
MOM		8415.8	3452
FEM	D-CGN	1360	283.0
	SSOR-CGN	1031	315.5
	FSAI-CGN	585	431.5

In the followings, the accuracy of the FEM algorithm for targets placed far away from the interface is tested. The same PEC sphere is placed 3.5λ below the interface. The simplified FEM model in Fig. 2 is used. The computation region is uniformly discretized with 0.05λ mesh size. For comparison, the FEKO is meshed with 0.05λ, the number of triangle meshes is 13868. The comparison of FEM results with the simulated results by FEKO is depicted in Fig. 7. Good agreements are found. This showed that 3D FEM can accurately simulate the targets placed far away from the air-earth interface. In this example, the CPU time used by FEKO is 8213 sec, the peak memory is 3.238 GB. The CPU time used by FEM with FSAI-CGN solver is 366 sec, the memory is 431.5 MB.

The third example tested is the bistatic scattering of a $2.5\lambda\times2.5\lambda\times0.2\lambda$ PEC brick buried below the earth. Assuming the electric constant of the earth is $\varepsilon_r=4.0-0.2j$, $\mu_r=1.0$. The incident angle is $\theta=0^o$, $\varphi=0^o$. In this case, the problem is uniformly discretized with the average mesh size 0.05λ. As a result, 802720 tetrahedrons and 954211 unknown edges are generated. Figure 8 showed the VV polarized bi-static RCS results simulated with 3D FEM and with FEKO. In this example, the mesh is 0.05λ in FEKO, the number of patches is

16220. The CPU time used by FEKO is 7591 sec. The peak memory is 4.4 GB. The CPU time used by FEM with FSAI-CGN solver is 1428 sec, the memory used is 616.5 MB.

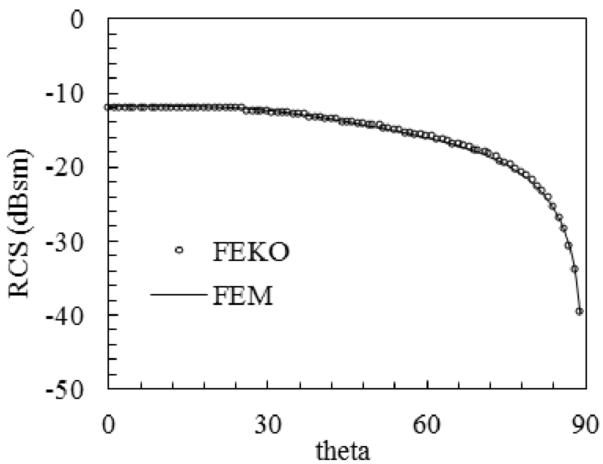

Fig. 7. Bi-static radar cross sections of the PEC sphere buried 3.5λ below the earth.

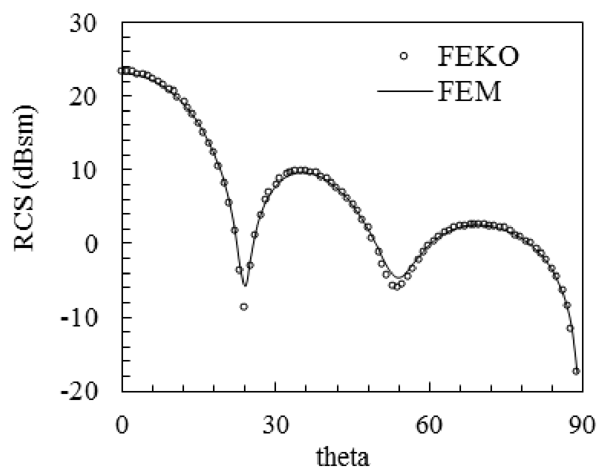

Fig. 8. Bi-static radar cross sections of a $2.5\lambda\times2.5\lambda\times0.2\lambda$ PEC cube buried below the earth.

As have been noted above, one advantage of FEM is that it can deal with complex dielectric materials. However, dielectric media buried under earth is hard to be simulated with FEKO. To validate the accuracy of FEM in simulating dielectrics, here a compound cube buried 0.1λ below the earth is computed. The cube is formed by a $2.5\lambda\times2.5\lambda\times0.2\lambda$ dielectric cube placed above the $2.5\lambda\times2.5\lambda\times0.2\lambda$ PEC cube. The permittivity of the dielectric cube is equal to the permittivity of the earth, i.e., $\varepsilon_r = 4.0 - 0.2j$. The incident angle is θ=0°, φ=0°. In Fig. 9, the RCS results of the compound cube and the RCS results of the PEC cube are compared, two results agreed quite well.

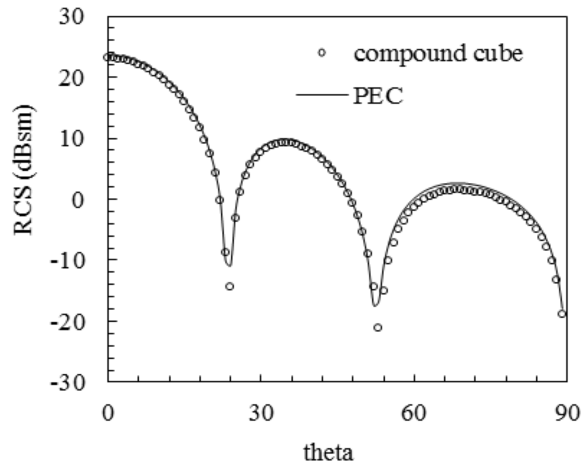

Fig. 9. Bi-static radar cross sections of the PEC cube and the compound cube buried 0.1λ below the earth.

Next, we assume the interface is not planar. There are many $0.1\lambda\times0.1\lambda\times0.2\lambda$ cavities uniformly distributed on the interface above the PEC brick, the distance between two nearest cavities is 0.1λ. The illustrated figure is shown in Fig. 10. The VV polarized Bi-static RCS results simulated with 3D FEM when the incident angle is θ=0° is shown in Fig. 11.

This problem cannot be simulated by FEKO. For comparison, the results for planar interface are also drawn in the figure. Two results are quite similar, but the RCS value for the interface with many cavities is a little smaller than that for plane interface in most angles. This is reasonable because the incident angle is perpendicular to the interface.

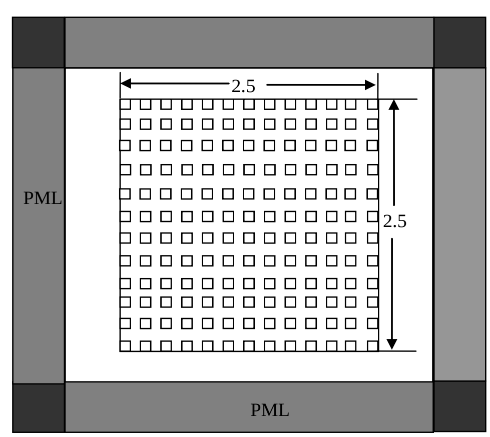

(a) Top view

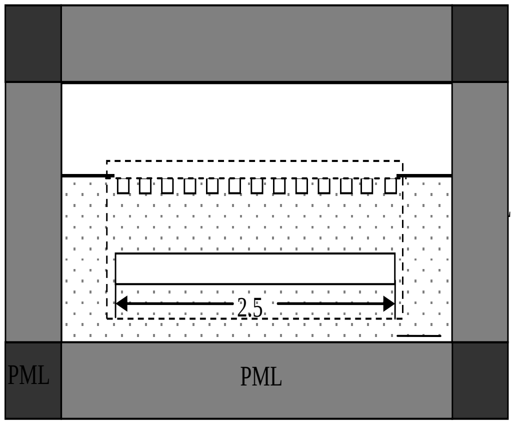

(b) Side view

Fig. 10. Illustration of the FEM computational domain of a PEC brick placed below the rough interface.

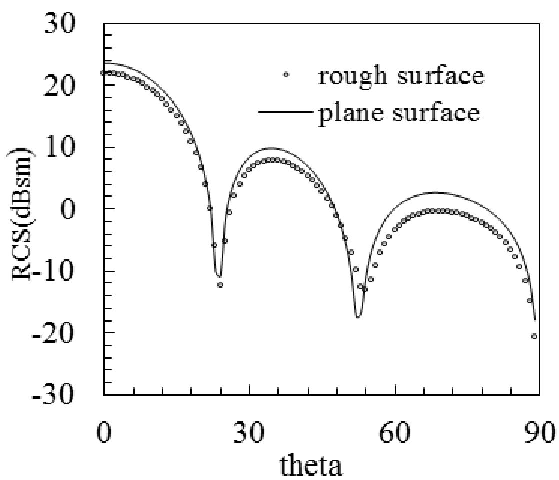

Fig. 11. Bi-static radar cross sections of the $2.5\lambda\times2.5\lambda\times0.2\lambda$ PEC brick when the air-earth interface is rough.

The next example tested is the bistatic scattering of a $5\lambda\times5\lambda\times5\lambda$ brick buried 0.3λ below the earth. Assuming the electric constant of the earth is $\varepsilon_r = 4.0-0.2j$, $\mu_r = 1.0$. The incident angle is θ=0^o, φ=0^o. Firstly, assuming the brick is PEC. The problem is uniformly discretized with the average mesh size 0.05λ, the generated tetrahedrons and unknown edges are respectively 4,072,000 and 4,662,546. Secondly, the brick is assumed to be dielectric with electric constant ε_r=2.0, μ_r=1.0. With mesh size 0.05λ, a total of 9,072,000 tetrahedrons and 10,752,846 unknowns are obtained. Figure 12 showed the simulated bi-static RCS results with VV polarization. As it is hard to solve a problem with such large electric-size by FEKO and dielectric media buried under earth cannot be simulated by FEKO, only 3D FEM results are given in the figure.

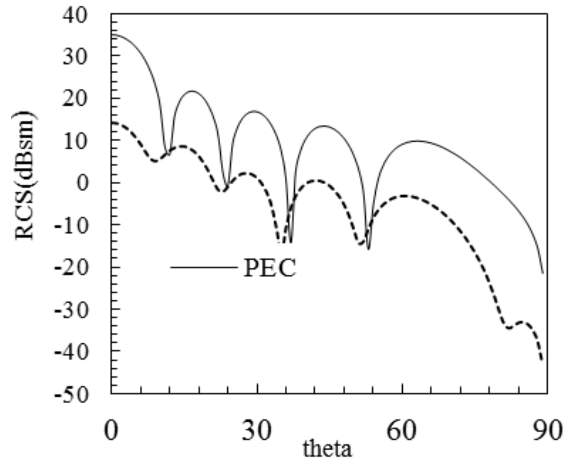

Fig. 12. Bi-static radar cross sections of a $5\lambda\times5\lambda\times5\lambda$ PEC brick and a dielectric brick buried 0.3λ below the earth.

The last example is the simulation of a cloak half buried below the earth. The relative permittivity of the earth is $\varepsilon_r = 1.5-0.2j$. Assuming the inner and outer boundary of the cloak are descripted by:

$$R_1 = 0.2+0.05\cos(3\theta)+0.01\cos(\theta),$$

$$R_2 = 0.3+0.05\cos(3\theta)+0.01\cos(\theta).$$

The relative permittivity and permeability of the cloak can be deduced with method described in [25-26] according to the above contour equations. In cylindrical coordinates, they are described by:

$$\bar{\bar{\varepsilon}}_r = \left[\varepsilon_{r,1}\,\mathrm{sgn}(z)+(\varepsilon_{r,2})\mathrm{sgn}(-z)\right]JJ^T/|J|,$$

$$\bar{\bar{\mu}}_r = JJ^T/|J|,$$

where $\varepsilon_{r,1}$ and $\varepsilon_{r,2}$ is the relative permittivity of media 1 and media 2, other parameters are defined by:

$$\mathrm{sgn}(z) = \begin{cases} 0 & z \le 0 \\ 1 & z > 0 \end{cases},$$

$$J_{xx} = cos^2\varphi sin\theta(R_3 sin\theta + R_4/rcos\theta) + (sin^2\varphi + cos^2\varphi cos^2\theta)r'/r,$$

$$J_{xy} = \sin\theta\sin(2\varphi)(\mathrm{R}_4\cos\theta\text{-}\mathrm{R}_1\sin\theta)/(2\mathrm{r}),$$

$$J_{xz} = \text{-}\cos\varphi\sin\theta(\mathrm{R}_1\cos\theta+\mathrm{R}_4\sin\theta)/\mathrm{r},$$

$$J_{yx} = J_{xy},$$

$$J_{yy} = sin^2\varphi sin\theta(R_3 sin\theta + R_4/rcos\theta) + (cos^2\varphi + \cos^2\theta\sin^2\varphi)r'/r$$

$$J_{yz} = \text{-}\sin\varphi\sin\theta(\mathrm{R}_1\cos\theta + \mathrm{R}_4\sin\theta)/\mathrm{r}$$

$$J_{zx} = \cos\varphi\cos\theta(\mathrm{R}_4\cos\theta\text{-}\mathrm{R}_1\sin\theta)/\mathrm{r}$$

$$J_{zy} = \cos\theta\sin\varphi(\mathrm{R}_4\cos\theta\text{-}\mathrm{R}_1\sin\theta)/\mathrm{r}$$

$$J_{zz} = cos\theta(R_3 cos\theta - R_4/rsin\theta) + r'/rsin^2\theta$$

With R_3, R_4 defined by:

$$R_3 = \frac{R_2 - R_1}{R_2}.$$

$$R_4 = \frac{\left[r' - R_1\right] \mathrm{R}_1\, dR_2 / d\theta}{R_2\left[R_2 - R_1\right]} - \frac{\left[r' - R_2\right] \mathrm{R}_2\, dR_1 / d\theta}{R_2\left[R_2 - R_1\right]}.$$

The value of the relative permittivity and permeability of the cloak in Cartesian coordinates can be obtained using the above formulation. Assuming the frequency of the incident plane wave is 1.0 *GHz*. The incident angle is $\theta = 30^o$, φ=0^o. The problem is discretized with the average mesh size 0.05λ in free space and 0.02λ in the cloak. To investigate the effect of the cloak, the electric field distribution near the coordinate origin is plotted in Fig. 13. Figure 13 (a) is the electric field distribution without cloak. Figure 13 (b) is the electric field distribution with cloak. As can be seen, the field outside the cloak is almost unchanged. This agrees with the theoretical results.

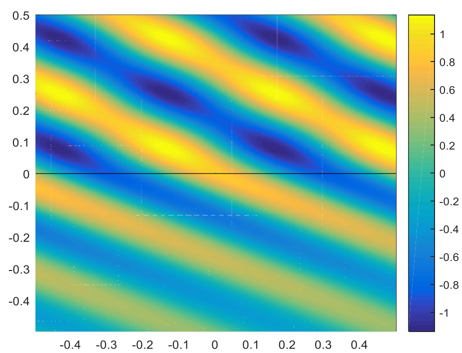

(a)

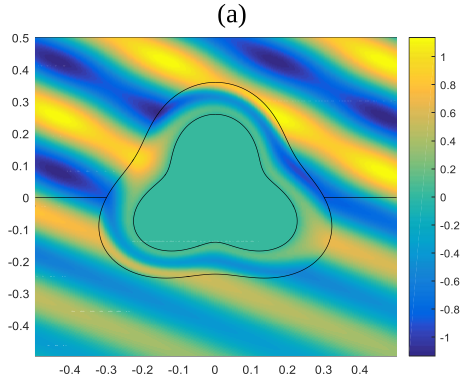

(b)

Fig. 13. The electric field distribution near the origin in the xoz plane when the plane wave incident from air to the loss media with the incident angle 30°. (a) Without the existence of the cloak, and (b) with the existence of the cloak.

VI. CONCLUSION

In this paper, the finite element method is used to analyze the scattering characteristics of 3D targets in the presence of air-earth interface. The FEM model for different cases including the targets placed near the interface, far away from the interface, and the interface is partially rough surface is discussed in the paper. The numerical results showed that the algorithm is very accurate and powerful for 3D targets in the presence of air-earth interface.

ACKNOWLEDGMENT

This work is supported in part by the Natural Science Foundation of Jiangsu Province under Grant BK20130854, in part by the Fundamental Research Funds for the Central Universities under Grant 2013B01914, in part by the National Science Foundation of China under Grant U1531101.

REFERENCES

[1] H. A. David, “Electromagnetic scattering by buried objects of low contrast,” *IEEE Trans, Geosci. Remote Sens*., vol. 26, pp. 195-203, 1988.

[2] N. Geng, A. Sullivan, and L. Carin, “Multilevel fast multipole algorithm for scattering from conducting targets above or embedded in a lossy half space,” *IEEE Trans, Geosci. Remote Sens*., vol. 38, pp. 1567-1579, 2000.

[3] Z. J. Liu, R. J. Adams, and L. Carin, “Well-conditioned MLFMA formulation for closed PEC targets in the vicinity of a half space,” *IEEE Trans. Antennas Propagat*., vol. 51, pp. 2822-2829, 2003.

[4] T. J. Cui and W. C. Chew, “Fast algorithm for electromagnetic scattering by buried 3-D dielectric objects of large size,” *IEEE Trans. Geosci. Remote Sens*., vol. 35, pp. 2597- 2608, 1999.

[5] B. Guan, J. F. Zhang, X. Y. Zhou, and T. J. Cui, “Electromagnetic scattering from objects above a rough surface using the method of moments with half-space green’s function,” *IEEE Trans. Geosci. Remote Sens*., vol. 47, pp. 3399-3405, 2009.

[6] J. Li, L. X. Guo, and H. Zeng, “FDTD investigation on bistatic scattering from a target above two-layered rough surfaces using UPML absorbing condition,” *Progress in Electromagnetics Research*, vol. 88, pp. 197-211, 2008.

[7] K. Demarest, R. Plumb, and Z. B. Huang, “FDTD modeling of scatterers in stratified media,” *IEEE Trans. Antennas Propagat.*, vol. 43, pp. 1164-1168, 1995.

[8] P. B. Wong, G. L. Tyler, J. E. Baron, et al., “A three wave FDTD approach to surface scattering with applications to remote sensing of geophysical surfaces,” *IEEE Trans. Antennas Propagat.*, vol. 44, pp. 504-514, 1996.

[9] J. M. Jin, *The Finite Element Method in Electromagnetics*. Wiley, New York, 1993.

[10] A. Aghabarati and J. P. Webb, “An algebraic multigrid method for the finite element analysis of large scattering problems,” *IEEE Trans. Antennas*

Propagat., vol. 61, no. 2, pp. 809-817, 2013.

[11] X. C. Wei, E. P. Li, and Y. J. Zhang, "Efficient solution to the large scattering and radiation problem using the improved finite-element fast multipole method," *IEEE Trans. Magn*., vol. 41, pp. 1684-1687, 2005.

[12] W. G. Facco, E. J. Silva, A. S. Moura, N. Z. Lima, and R. R. Saldanha, "Handling material discontinuities in the generalized finite element method to solve wave propagation problems," *IEEE Trans. Magn*., vol. 48, pp. 607-610, 2012.

[13] S. Caorsi and M. Raffetto, "Perfectly matched layers for the truncation of finite element meshes in layered half-space geometries and applications to electromagnetic scattering by buried objects," *Microwave Opt. Technol. Lett.*, vol. 19, pp. 427-434, 1998.

[14] O. Ozgun and M. Kuzuoglu, "Monte Carlo-based characteristic basis finite-element method (MC-CBFEM) for numerical analysis of scattering from objects on/above rough sea surfaces," *IEEE Trans. Geosci. Remote Sens*., vol.50, pp. 769-783, 2012.

[15] D. H. Han, A. C. Polycarpou, and C. A. Balanis, "Ground effects for VHF/HF antennas on helicopter airframes," *IEEE Trans. Antennas Propagat*., vol. 49, pp. 402-412, 2001.

[16] E. Simsek, J. Liu, and Q. H. Liu, "A spectral integral method and hybrid SIM/FEM for layered media," *IEEE Transactions on Microwave Theory and Techniques*, vol. 54, no. 11, pp. 3878-3884, 2006.

[17] T. Eibert, Y. Erdemli, and J. Volakis, "Hybrid finite element-fast spectral domain multilayer boundary integral modeling of doubly periodic structures," *IEEE Transactions on Antennas and Propagation*, vol. 51, no. 9, pp. 2517-2520, Sept. 2003.

[18] R. Xu, L. Guo, and X. Meng, "Analysis of scattering from dielectric rough surfaces by hybrid FEM/BIE," *Progress In Electromagnetics Research M*, vol. 34, pp. 107-116, 2014.

[19] L. Guo and R. Xu "An efficient multiregion FEM-BIM for composite scattering from an arbitrary dielectric target above dielectric rough sea surfaces," *IEEE Transactions on Geoscience and Remote Sensing*, vol. 53, no. 7, pp. 3885-3896, 2015.

[20] B. M. Irons, "A frontal method solution program for finite element analysis," *Int. J. Numer. Meth. Eng*., vol. 2, pp. 5-32, 1970.

[21] Y. Saad, *Iterative Methods for Sparse Linear Systems*. PWS Publishing Company, Boston, 1995.

[22] M. Benzi, "Preconditioning techniques for large linear systems: A survey," *Journal of Computational Physics*, vol. 182, pp. 418-477, 2002.

[23] R. S. Chen, X. W. Ping, E. K. N. Yung, C. H. Chan, et al., "Application of diagonally perturbed incomplete factorization preconditioned conjugate gradient algorithms for edge finite element analysis of Helmholtz equations," *IEEE Trans. Antennas Propagat*., vol. 54, pp. 1604-1608, 2006.

[24] X. W. Ping and T. J. Cui, "The factorized sparse approximate inverse preconditioned conjugate gradient algorithm for finite element analysis of scattering problems," *Progress In Electromagnetics Research*, vol. 98, pp. 15-31, 2009.

[25] D. Schurig, J. B. Pendry, and D. R. Smith, "Calculation of material properties and ray tracing in transformation media," *Opt. Express*, vol. 14, pp. 9794-9804, 2006.

[26] C. Li, K. Yao, and F. Li, "Invisibility cloaks with arbitrary geometries for layered and gradually changing backgrounds," *J. Phys. D: Appl. Phys*., vol. 42, 185504, 2009.

Xuewei Ping received the B.S., M.S., and Ph.D. degrees from Nanjing University of Science and Technology, Nanjing, China, in 2001, 2004, and 2007, respectively. Since Dec 2012, he has been a Lector of HoHai University. His research interests include computational electromagnetics, radar cross-section analysis, electromagnetic design and analysis of magnetic resonance imaging components.